JOURNAL OF CATALYSIS 124, 116–126 (1990)

Enthalpy and Entropy of H_2 Adsorption on Rh/Al_2O_3 Measured by Temperature-Programmed Desorption

ANGELOS M. EFSTATHIOU[1] AND CARROLL O. BENNETT[1]

Department of Chemical Engineering, University of Connecticut, Storrs, Connecticut 06268

Received July 20, 1989; revised January 30, 1990

Temperature-programmed desorption spectroscopy under pseudo-equilibrium conditions has been used to obtain the coverage dependence of the heat and entropy of hydrogen adsorption for a 5-wt% Rh/Al_2O_3 catalyst. This method is considered to be more convenient than volumetric or flow methods. The latter require more effort to obtain various isotherms and isobars, from which the heat and entropy of adsorption are obtained in a manner similar to that in this study. Extrapolation of the heat and entropy of adsorption to zero coverage yields values of 24 kcal/mol and 38 cal/mol-K, respectively. For the former value, a binding energy of 64 kcal/mol is obtained, which is comparable to reported values for a polycrystalline Rh surface. © 1990 Academic Press, Inc.

INTRODUCTION

Temperature-programmed desorption (TPD) spectroscopy on supported catalysts and single crystals is often used for obtaining information on the nature of the interaction of adsorbed species with each other and with the surface (*1, 2*). When correctly performed under vacuum conditions, kinetic data are obtained. For supported catalysts at atmospheric pressure, thermodynamic rather than kinetic data may result, as discussed in the present work.

From the results of TPD from flat surfaces under vacuum conditions, by proper procedures (*3–5*), the frequency factor ν and the activation energy of desorption E can be obtained as a function of surface coverage θ. The methods of Redhead (*6*) and of Chan *et al.* (*7*) are suitable if ν and E do not vary with θ, and other methods suitable when ν and E vary with θ have appeared (*8–10*). For metal-supported catalysts, much of the older data is probably useful only in a qualitative way, not for obtaining good values of E and ν or $\Delta H°$ and $\Delta S°$ of adsorption. This is because (a) various transport effects may considerably alter the peak maximum temperature T_M (*11–15*); (b) procedures based on the peak shape may give erroneous results (*16*); and (c) to extract desorption kinetic parameters from TPD spectra through simulation, the sticking coefficient for adsorption must be known (*17*). The latter is generally not known for metal-supported catalysts and is typically obtained from surface science studies.

For TPDs at atmospheric pressure, readsorption occurs, and it was suggested that adsorption and desorption are in quasi-equilibrium during the TPD (*11*). This means that the kinetic quantities $\nu(\theta)$ and $E(\theta)$ cannot be obtained; the appropriate parameters are those related to equilibrium, $\Delta S°(\theta)$ and $\Delta H°(\theta)$. These equilibrium quantities have been obtained by measurement of equilibrium isobars and were observed to vary as a function of θ (*18*). Since isobar measurements are tedious to perform, there is an incentive to establish a method to obtain $\Delta S°(\theta)$ and $\Delta H°(\theta)$ from TPD measurements. Lee and Schwarz (*19*), using TPDs for various initial coverages, have extracted desorption kinetic parameters as a function of coverage. The method (*19*) has also been used by Weatherbee and Bartholomew (*20*). In the present study,

[1] To whom correspondence should be addressed.

0021-9517/90 $3.00

however, a different procedure is used to establish an initial coverage. This procedure will permit us to measure the equilibrium constant $K(\theta, T)$ from "equilibrium" TPDs, so that $\Delta H°(\theta)$ and $\Delta S°(\theta)$ can be evaluated. The assumption of quasi-equilibrium will be justified over the necessary span of operating parameters.

This paper will discuss first the appropriate design of the TPD experiment based on criteria already established in the literature (*13*) and then show how to determine $\Delta H°(\theta)$ and $\Delta S°(\theta)$ for H_2 chemisorption on a Rh/Al_2O_3 catalyst.

EXPERIMENTAL

Catalyst. The preparation and characterization of the 5.2 wt% Rh/Al_2O_3 have been previously reported in detail (*21, 22*). Table 1 summarizes the properties of the catalyst related to this study. The catalyst sample, before the initiation of the TPD studies, has been treated with 1 atm H_2 (35 ml/min, ambient) at 623 K for 20 h, and during the TPD studies with 30% H_2/Ar at 623 K for 1 h, whenever appropriate. Chemisorption with 1 atm H_2 at 310 K before and after the TPD studies revealed that no sintering of the Rh crystallites had occurred. The density of the pelletized catalyst was determined by using the pycnometer method (*23*).

Reactor–flow system. A once-through stainless-steel microreactor of 0.5 ml internal nominal volume was used (*24*). The behavior of this reactor was that of a CSTR, with a mixing time of about 1 s for 30 ml/min (ambient). The flow system was the same as described previously (*24, 25*). Mixtures of H_2/Ar were prepared from zero grade H_2 and Ar (Aero All-Gas Co.) in a mixing panel. A dilute mixture of H_2 in Ar (3600 ppm H_2) was used to calibrate the mass spectrometer (MS). Zero grade H_2 and Ar carrier gases were further purified as described elsewhere (*24*). Heating rates were produced by using a temperature programmer (Bendix), to better than 2% reproducibility.

Mass spectrometry. The high resolution MS (Nuclide 12-90-G) produced a flat-topped peak for the H_2^+ ion beam, eliminating any signal change from reasonable drifts in the magnetic and ion acceleration potential fields. Sensitivity and the amount of background H_2 were recorded before and after each TPD run. Data acquisition and integration of the MS response have been performed as described in detail (*21, 22*). The contribution of H_2O to the mass number 2 was estimated to be less than 1% under the ionization conditions used. Calibration of the MS for H_2O was described previously (*22*).

Blank experiments. During the reduction step at 623 K with 1 and 0.3 atm H_2, some dissolution of hydrogen in the stainless-steel reactor was observed. After the reduction step, the reactor was purged at 673

TABLE 1

Properties of the Rh/Al_2O_3 Catalyst

Property	Value	Method	Ref.
Composition	5.2 wt%	Atomic absorption	(*22*)
Fraction exposed	0.12	H_2 chemisorption[a]	(*18, 22*)
Particle size	11 nm	H_2 chemisorption,[b] XRD	(*22*)
Al_2O_3 surface area	110 ± 10 m^2/g	BET	(*22*)
Rh surface area	2.88 m^2/g	H_2 chemisorption	(*22*)
Catalyst pellet size	0.03 cm	Sieving procedure	(This study)
Catalyst pellet density	3.35 g/cm^3	Pycnometer	(This study)

[a] Extrapolating the linear part of the isotherm to zero pressure and assuming $H/Rh_s = 1.0$.
[b] Assuming spherical Rh particles.

K with Ar for 5 min, closed off (by using a six-way chromatographic valve (*25*)) for 5 min, and then opened again for another 5-min purge. This cycle was repeated several times until the H_2 concentration at 673 K was less than 50 ppm. When the temperature in flowing Ar was then reduced to 623 K, the hydrogen signal reached the baseline.

Any residual adsorbed water on the alumina support, after the 20-h reduction step and the subsequent desorption of dissolved hydrogen from the reactor, should not contribute to the subsequent observed H_2 TPDs (cracking effect). To confirm this fact, after the end of the Ar purge procedure in the previous paragraph, the reactor was cooled to about 323 K and a TPD in Ar for $m/e = 18$ was performed. No water was detected at temperatures below 643 K.

A blank run was made by using the alumina support (95 mg) alone. For the same pretreatment and adsorption conditions for Rh/Al_2O_3 as presented before, the support alone yielded only insignificant amounts of H_2 chemisorption (less than 1% of chemisorption on Rh/Al_2O_3).

Designing a TPD experiment free of mass transfer effects. The various criteria proposed by Demmin and Gorte (*13*) will be used in this work. The most difficult criteria to satisfy are (a) assuring that the TPD reactor behaves as a mixed flow reactor, CSTR (criterion is the Peclet number), and (b) the ratio of carrier gas flow rate to the rate of diffusion inside the catalyst particle. In order to avoid excessive gradients in the gas phase, the Peclet number should be <0.1 (*13*). A mass of catalyst W of 100 mg and a bed density ρ_b of 1 g/cm^3 lead to a bed volume V_b of 0.1 cm^3. A catalyst bed diameter of 1 cm leads to a bed length Z of 0.13 cm. Experimentally, this is about as far as it is reasonable to go for achieving a shallow bed. The flow rate q can be no smaller than the required leak rate into the mass spectrometer (ca. 0.2 cm^3/s). The remaining factor in the Peclet number is the eddy diffusivity in the bed, D_b, which is expected to be higher than the ordinary molecular diffusivity of about 0.1 cm^2/s. Obtaining an accurate estimate of D_b is difficult. The above values lead to a value for the Peclet number ≤ 0.34. Proper reactor design, details of which were given (*24*), results in a D_b much greater than 0.1. Since very good CSTR behavior has been observed for many transient experiments (*24–26*), it is clear that $D_b \gg 0.1$ cm^2/s. Thus, the Peclet criterion appears to be satisfied, but only with careful selection of the experimental conditions.

The next criterion to consider is the ratio of carrier gas flow rate to the rate of diffusion inside the catalyst particle. This ratio is proportional to the square of the thickness l of the catalyst particle and inversely proportional to the intraparticle effective diffusivity, D_p. The lowest practical value of l is necessary to keep the value of this criterion below 0.05 (*13*). With a particle density ρ_p of 2.0 g/cm^3, q of 0.2 cm^3/s, W of 0.1 g, l of 0.15 mm, and D_p of about 0.02 cm^2/s, the criterion value becomes 0.045. Again we see how difficult it is to achieve gradientless conditions.

Once the two criteria mentioned above have been satisfied, there is no problem satisfying the other criteria (*13*). Two criteria concerning readsorption must also be considered (*13*), and the values calculated for these are much greater than the limiting values of 1.0 suggested (*13*). There is no way to satisfy these criteria under atmospheric pressure, while retaining acceptable values of the two criteria mentioned in the previous paragraphs. Therefore, we shall try to work under conditions for which *pseudo-equilibrium* exists during the TPDs. The validity of this assumption will be demonstrated after the presentation of the experimental results.

A gradientless TPD experiment. The experimental parameters used to calculate the various criteria suggested for a gradientless TPD (*13*) were the following: $q = 0.39$–0.60 cm^3/s between 393 and 603 K; $Z = 0.1$ cm; $V_b = 0.06$ cm^3; $D_b = 1.0$ cm^2/s; $l = 0.015$ cm; $\rho_p = 3.35$ g/cm^3; $D_p = 0.02$ cm^2/s; $W =$

0.095 g; $\varepsilon_b = 0.80$; $\varepsilon_p = 0.5$; $V = 0.34$ cm^3; $\beta = 0.6$ K/s; $T_i = 390$ K; $T_f = 610$ K. Here, ε_b is the porosity of the bed (applied to the whole CSTR), and ε_p the porosity of the catalyst particle. Also, T_i and T_f are the starting and final TPD peak temperatures, respectively. The physical meanings of the other parameters, not mentioned before, are given in the Appendix. The values of 0.065–0.102, 0.155–0.242, 0.0019–0.0012, and 1.53×10^{-5} were calculated for the four criteria (*13*): the Peclet number, the ratio of carrier gas flow rate to the rate of diffusion, the ratio of the average residence time of the carrier gas to the time span of the experiment, and the ratio of the diffusion time constant to the time span of the experiment, respectively. As already mentioned, the first two criteria are the most difficult to satisfy.

Pseudo-equilibrium TPD experiment. The Appendix describes the mathematical procedure followed to analyze the TPD results of this study. As indicated, the assumptions made concerning the ratios of accumulation/effluent and effluent/readsorption terms of the CSTR material balance can lead to a TPD with a rate of readsorption (within the catalyst particle) very close to the rate of desorption, leading therefore to a small net rate of desorption (rate of removal) of the adsorbate from the surface. This is visualized as representing a pseudo-equilibrium condition. The achievement of such condition (for the TPDs of this study) will be verified after we present the experimental TPDs to follow.

RESULTS

Equilibrium chemisorption. The equilibrium chemisorption results, obtained by a method already described (*18*), at 300 K for various H_2 pressures (isotherm) are presented in Fig. 1. The adsorption time was 20 min, the flow rate was 40 ml/min (ambient), and the amount of catalyst was 0.69 g. The reproducibility of this flow technique was between 3–5%. Triangles in Fig. 1 correspond to adsorption time of 20 min and 15 h also. This result indicates that under the experimental conditions used the system achieves its equilibrium state within 20 min. Extrapolation of the isotherm (H/Rh curve) to zero pressure leads to a rhodium fraction exposed, FE, of 0.12, for the value of $H/Rh_s = 1.0$ suggested by Scholten *et al.* (*27*). A Temkin isotherm provides the best fit to the experimental data of Fig. 1.

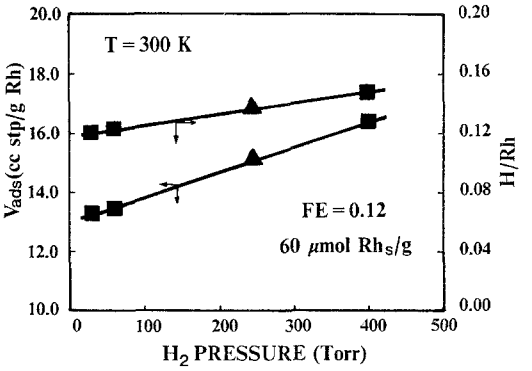

FIG. 1. H_2 equilibrium chemisorption isotherm for the 5.2-wt% Rh/Al_2O_3 catalyst. (■) 20 min adsorption time; (▲) 20 min and 15 h adsorption time.

Temperature-programmed desorption. The primary goal of this study was to establish an experimental procedure that uses on-line mass spectrometry and TPD spectroscopy to obtain the heat and entropy of adsorption as a function of coverage. Having designed a TPD experiment to practically eliminate mass transfer falsifications, the establishment of an initial coverage varying from $\theta_i = 1.0$ (a monolayer value) to a practical small value $\theta_i = 0.1$ can be achieved in various ways. For instance, Lee and Schwartz (*19*) used the pulse method at room temperature. Chin and Bell (*17*) used a flow method for adsorption and varied the evacuation time at room temperature. The simulations of Balkenende *et al.* (*16*), for the case of a dynamic adsorption, show that adsorption occurs as a front which gradually penetrates the catalyst pellets. When this is done near room temperature, the rate of desorption is small (due to the large heat of adsorption) and the rate of

TABLE 2

Experimental Conditions for Establishing Uniform Initial Coverage θ_i

θ_i	Purge T (K)	Purge time (min)
0.20	353 → 413	2.0
	413	7.0
	413 → 423	3.0
	423 → 448	3.0
	448 → 388 (T_i)	4.5
0.32	353 → 413	5.0
	413 → 370 (T_i)	4.5
0.48	353 → 413	4.0
	413 → 361 (T_i)	6.0
0.62	353 → 413	3.0
	413 → 358 (T_i)	7.0
0.70	353 → 383	1.5
	383	10.0
	383 → 338 (T_i)	4.5
0.80	353 → 373	1.0
	373	10.0
	373 → 333 (T_i)	3.8
0.92	353 → 373	1.0
	373	5.0
	373 → 337 (T_i)	3.5
1.05	353	5.0
	353 → 333 (T_i)	2.0

adsorption high, producing a slow redistribution of the adsorbate over the catalyst surface. This results in a nonuniform initial surface coverage. However, it was demonstrated (*16*) that when adsorption is performed at elevated temperatures to increase the rate of desorption, the surface coverage becomes more homogeneous. The effect of adsorbate supply on the establishment of a homogeneous surface coverage during adsorption was also discussed (*16*).

When the adsorption occurs at 310 K (30 min adsorption), we have found that an isothermal Ar purge (310 K, 18 ml/min, 15 min) removes only 0.125 and 0.10 of a monolayer, for the cases of 1 atm and 0.3 atm H_2 adsorption, respectively. The initiation of a TPD with 0.6 K/s heating rate, after the isothermal purge, creates a single TPD peak with a peak maximum temperature T_M of 408 K and an amount equal to 1.39 and 1.12 of a monolayer, for the 1 atm and 0.3 atm H_2 adsorption cases, respectively. No desorption was measured above 593 K. These results are consistent with those shown in Fig. 1.

The results mentioned above were used to determine the conditions that should yield initial coverages of only strongly adsorbed hydrogen. Table 2 gives the experimental conditions applied. The adsorption temperature before the initiation of any TPD run was 353 K, the adsorbate gas was 30% H_2/Ar, the flow rate was 35 ml/min (ambient), and the adsorption time was 30 min. These adsorption conditions, in accordance with the results of Balkenende *et al.* (*16*), are believed to have created a homogeneous initial surface coverage. By applying various purge times in pure Ar at a selected temperature range after the adsorption step, appropriate initial surface coverages were created. Note that at the beginning of any TPD run, baseline was achieved; no H_2 was desorbing in the Ar flow at the appropriate T_i.

Figure 2 presents the TPD profiles obtained according to the conditions of Table 2. As the initial coverage decreases, a shift in the peak maximum temperature, T_M, to-

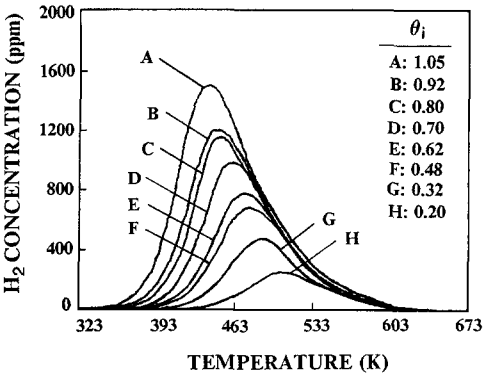

FIG. 2. Experimental H_2 TPDs for the initial coverages listed in Table 2.

TABLE 3

Peak Maximum Properties of the Various TPDs of Fig. 2

θ_i	T_M (K)	y_M (ppm)	θ_M
0.20	508	250	0.124
0.32	488	490	0.195
0.48	478	670	0.298
0.62	473	770	0.380
0.70	465	960	0.470
0.80	453	1135	0.520
0.92	448	1185	0.635
1.05	438	1480	0.645

ward higher T_s is observed, along with a decrease in the maximum gas phase concentration y_M. This behavior is summarized in Table 3. From the calculated θ_M values, some asymmetry in the peaks is observed, and this is more pronounced as θ_i increases.

Determination of $\Delta H°(\theta)$ *and* $\Delta S°(\theta)$. The procedure that enables one to extract the heat and entropy of adsorption as a function of coverage from the TPD profiles of Fig. 2 is now presented. At a preselected temperature T_1, the gas phase mole fraction y and the coverage θ must be determined. The y is obtained from the direct measurement, and the coverage θ is obtained by integrating the TPD profile between T_1 and the final temperature T_f, where baseline is obtained. In Fig. 2 one can visualize perpendicular lines at a certain T_1, intersecting the TPD profiles. The values of y and θ obtained from this procedure are then used in Eq. (7) given in the Appendix, to calculate the corresponding equilibrium constant $K(\theta, T)$. These results are presented as ln K vs coverage in Fig. 3 for various preselected temperatures. In order to span the coverage range of $0.08 \leq \theta \leq 0.95$ indicated in Fig. 3 with enough data points, several attempts at selecting the T_s were necessary. This is because for certain temperatures and initial coverages only a few data points are obtained, since some K values obtained from different initial coverage curves may have the same value.

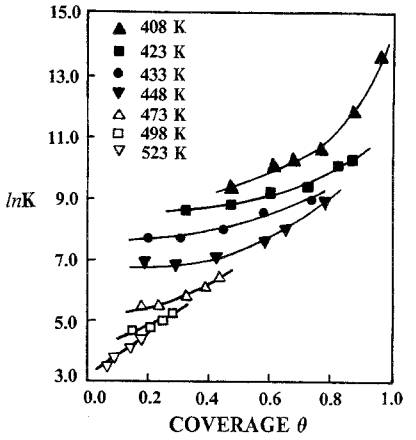

FIG. 3. Experimental equilibrium $K(\theta, T)$ values vs coverage for various temperatures.

From the curves of Fig. 3, the equilibrium values of K for different temperatures are obtained for a given coverage θ. This procedure generates the isosters (θ = const) for the pseudo-equilibrium chemisorption shown in Fig. 4. From Eq. (9) in the Appendix, the heat and entropy of adsorption can be determined as a function of coverage. During the treatment of the data of Fig. 2 it has been observed that for coverages below about 0.12 it is not possible to obtain reliable $\Delta H°$ and $\Delta S°$ values. This is because of the coincidence of all the TPD

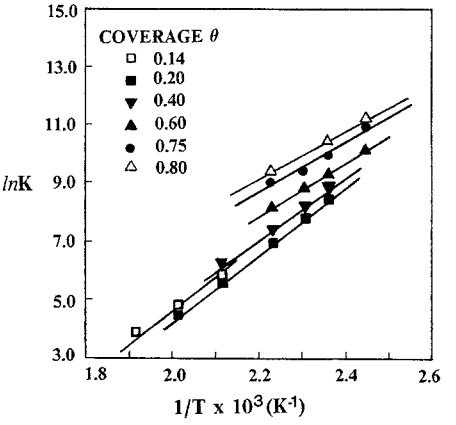

FIG. 4. Arrhenius plot of ln K vs $1/T$ for various coverages.

profiles at the high-temperature edge. The same observation has been made by Balkenende *et al.* (*16*). In addition, in order to obtain values for $\Delta H°$ and $\Delta S°$ for coverages greater than 0.8, experimental TPD profiles with initial coverages above a monolayer would be needed. The latter inevitably will include weakly held H_2, and the interpretation of results would be difficult.

Figure 5 clearly shows that both heat and entropy of adsorption *do vary* with coverage. For the Rh/Al_2O_3 catalyst of this study, $\Delta H°(\theta)$ decreases linearly from 22.5 kcal/mol to 15.3 kcal/mol in the range of $0.15 \leq \theta \leq 0.8$. For the entropy of adsorption the values of 36.2 and 15.6 kcal/mol-K were obtained at $\theta = 0.15$ and 0.80, respectively.

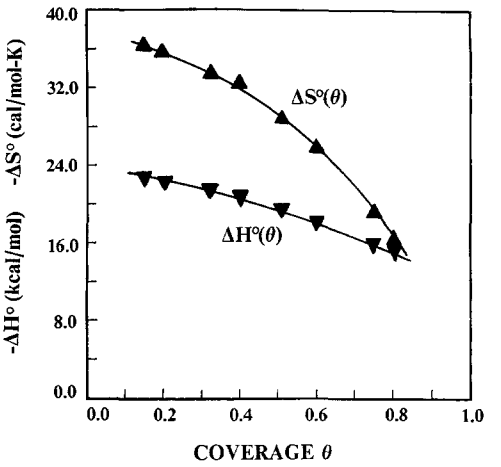

FIG. 5. Experimental heat of adsorption $\Delta H°(\theta)$ and entropy of adsorption $\Delta S°(\theta)$ for the 5.2-wt% Rh/Al_2O_3 catalyst.

Justification of pseudo-equilibrium during TPD. The assumptions made in deriving the equilibrium relationship (Eq. 7) are justified by examining two representative experimental TPD profiles. We have selected the TPDs of $\theta_i = 0.92$ and 0.48. The results are shown in Table 4. For these calculations the following parameters were used: $V = 0.34$ cm^3; $q_0 = 0.3$ cm^3/s; $\beta = 0.64$ K/s; $W = 0.095$ g; $\sigma = 7.9 \times 10^{-16}$ cm^2/Rh atom. It can be seen from these results that the two simplifications made are justified very well.

Nonactivated H_2 chemisorption. It is important to show that H_2 chemisorption on the Rh/Al_2O_3 catalyst was a nonactivated process, in order to be consistent with pseudo-equilibrium TPD. The following experiments were performed. The catalyst was treated with 30% H_2/Ar at 393 K for 20 min, cooled to 310 K in H_2/Ar, and left at

TABLE 4

Justification of the Model Simplifications for Pseudo-Equilibrium TPD Experiments

T (K)	Accum. term (moles/s) $\times 10^{12}$		Accum./effl.		$0.5k_a(1-\theta)^2WH$ (moles/s) $\times S_0^{-1}$		$S_0 >$ [c]	
408	22.7[a]	176.0[b]	0.027	0.036	585.6	32.2	2.1×10^{-6}	0.4×10^{-4}
423	53.2	177.0	0.034	0.019	589.2	65.8	2.1×10^{-6}	0.2×10^{-4}
433	86.5	136.4	0.028	0.010	619.5	136.7	2.0×10^{-6}	0.9×10^{-5}
448	93.7	9.0	0.018	0.001	679.9	245.8	1.8×10^{-6}	0.5×10^{-5}
473	7.7	107.5	0.001	0.009	903.2	635.4	1.4×10^{-6}	0.2×10^{-5}
498	46.1	64.2	0.006	0.008	1208.0	1004.3	1.0×10^{-6}	0.1×10^{-5}
523	54.4	51.5	0.012	0.010	1512.1	1291.7	0.8×10^{-6}	0.9×10^{-6}
548	11.2	22.6	0.005	0.010	1669.8	1554.4	0.7×10^{-6}	0.8×10^{-6}

[a] $\theta_i = 0.48$.

[b] $\theta_i = 0.92$.

[c] S_0 must be greater than the number indicated in the column, in order to have effluent/readsorption less than 1%.

this temperature for 30 min. The amount of H_2 chemisorption for this case was found to be 1.25 of a monolayer. The same result, within experimental error, has been obtained when the adsorption temperature was increased to 573 K followed by a slow cooling of the reactor to 310 K in a H_2/Ar flow. Therefore, for the temperature range of the TPDs of Fig. 2, it is clear that readsorption of H_2 must be considered as a nonactivated process.

DISCUSSION

Gradientless and pseudo-equilibrium TPD experiment. It has been shown in the present study that proper reactor design, leading to a CSTR performance, and the selection of appropriate experimental conditions, eliminating mass transfer effects and producing pseudo-equilibrium during TPD, can provide the means to extract the heat and entropy of adsorption as a function of coverage. The procedure adopted in this study is considered to be more convenient than methods leading to the measurement of isotherms and isobars. In this study, few TPD runs are required, minimizing therefore sintering problems that might occur, especially for small metal-supported catalysts, in volumetric or flow chemisorption methods.

The results of Table 4 clearly demonstrate that the two simplifications made, in deriving the equilibrium relationship (Eq. 7), are justified very well. The accumulation term during the TPD is less than 3% of the effluent term. Considering the effluent term to be less than 1% of the readsorption term, the initial sticking coefficient S_0 must be, in the worst case, greater than 0.4×10^{-4}. Edwards *et al.* (*28*), for the adsorption of H_2 on Rh filament in the pressure range of 2×10^{-8} to 2×10^{-6} Torr at 160 K, reported an $S_0 = 0.4 \pm 0.03$. Therefore, it appears that S_0 for the present study is significantly higher than all of the values in Table 4. Note, however, that there is no need to assume a specific value of S_0.

Weakly chemisorbed H_2. The results of H_2 chemisorption of Fig. 1 suggest the presence of weakly adsorbed H_2 above the monolayer quantity. Weakly chemisorbed H_2 prior to the TPDs of Fig. 2 amounted to only 7% of the total chemisorption performed at 310 K with 1 atm H_2. Bertucco and Bennett have studied the H_2 chemisorption on a 10 wt% Rh/SiO_2 (*18*). The weakly adsorbed H_2 was found to be about 10% of the total chemisorption (300 K, 1 atm H_2), similar to the present study. In contrast, Zakumbaeva and Omashev (*29*) found for a 5-wt% Rh/Al_2O_3 that 25% of the total adsorbed hydrogen desorbed isothermally at 300 K. However, it should be kept in mind that the amount of isothermally desorbed H_2 strongly depends on the experimental conditions used.

$\Delta H°(\theta)$ and $\Delta S°(\theta)$ of strongly chemisorbed H_2. The TPD results of Fig. 2 (coverages below a monolayer) must correspond to desorption of atomically adsorbed hydrogen. The heat of adsorption obtained (Fig. 5), equivalent to activation energies of desorption (nonactivated chemisorption), argue for the latter. The H_2 adsorption at 353 K and the procedures applied here to obtain various initial uniform coverages produced a single TPD peak. On the other hand, the heat of adsorption varied with coverage as well as the entropy of adsorption, in a manner similar to that observed in many previous studies on metal-supported catalysts (low $\Delta H°$ at high θ and high $\Delta H°$ at low θ) (*18–20, 29, 30*).

To explain the variation of $\Delta H°$ with coverage, studies on single crystal surfaces (*10, 31–33*) suggest that repulsive interactions between adsorbed species is one reason for such behavior. Reconstruction of the substrate during TPD may be another reason (*34*), but the Rh(111) surface, the most closely packed plane of this *fcc* metal, was found to be unreconstructed and unrelaxed to within 5% (*35*). A mobile precursor state of H_2 on Rh(111) during the desorption process was also suggested (*32*). When the points mentioned above are considered, the $\Delta H°(\theta)$ behavior observed here favors re-

pulsive interaction effects. Under the conditions of the experiments, a precursor state with some activation barrier must be ruled out. On the other hand, it is difficult to envision deconvolution of the TPD profiles observed (Fig. 2) to many adsorbed hydrogen states without creating severe broadness and/or multiple peaks. Nevertheless, there may exist a main Rh adsorption site that would give a high adsorption amount and a few other sites with low population, the energies of which are such that the overall desorption creates the profiles of Fig. 2. However, only a small difference in the H_2 desorption energy from polycrystalline Rh and Rh(111) was reported (*32, 41*). The entropy of adsorption $\Delta S°(\theta)$ for the H-Rh/Al_2O_3 of this study shows a drop by 20 cal/mol-K in the range of $0.15 \leq \theta \leq 0.80$. Such a drop is not unusual on single crystals (*32, 34, 36*) and on metal-supported catalysts (*30*). The estimated $\Delta H°(\theta)$ and $\Delta S°(\theta)$ values here conform to the criteria of Vannice *et al.* (*40*), and are in general agreement with Rh single-crystal surfaces and some other Rh-supported catalysts (*18, 32, 37, 39*). The binding energy of a hydrogen atom given by $E_{Rh-H} = 0.5\ (E_{H-H} + \Delta H°)$ can be calculated. Using $E_{H-H} = 104$ kcal/mol (dissociation energy of H_2) and $\Delta H° = 24.0$ kcal/mol for $\theta \rightarrow 0$, we estimate $E_{Rh-H} = 64$ kcal/mol. This value is comparable to that reported for Rh filament (60.5 kcal/mol) (*41*).

$\Delta H°$ of H_2 and CO in relation to their catalytic activity in the CO/H_2 reaction. Aspects of the relation between chemisorption and catalysis for H_2 and CO have been discussed (*42*). The TPD of CO for this catalyst, when adsorption occurred at 300 K with 9.9% CO/He, shows a main CO peak at $T_M = 463$ K ($\theta_i = 1.2$) with a low-temperature shoulder (*26*). In addition, steady-state kinetics (*26*) shows a decrease in the methanation rate when the H_2/CO ratio decreases from 9 to 1. Transient isotopic kinetics (*21, 26*) revealed that the Rh surface of this catalyst is covered mostly by undissociated CO in the temperature range 180–260°C for H_2/CO = 9. These matters are consistent with the findings of the present study, and with reported $\Delta H°$ values for CO chemisorption on Rh surfaces (*43, 44*). The CO chemisorption appears to be stronger than H_2 chemisorption on Rh surfaces and may be responsible for low turnover frequencies in CO hydrogenation.

CONCLUSIONS

A gradientless TPD experiment, with conditions that lead to pseudo-equilibrium throughout, is a powerful tool to provide the heat and entropy of adsorption of a given adsorbate as a function of coverage. Such information provides useful insight into the catalytic properties of a given adsorbate–substrate system. The heat of hydrogen adsorption for the 5 wt% Rh/Al_2O_3 was found to vary from 24 kcal/mol ($\theta \rightarrow 0$) to 16 kcal/mol ($\theta = 0.8$), and the entropy of adsorption from 38 cal/mol-K ($\theta \rightarrow 0$) to 16.0 cal/mol-K ($\theta = 0.8$). These values generally agree with H_2 chemisorption results reported for various Rh surfaces.

APPENDIX

For the gradientless conditions achieved in this study, the basic equation describing the TPD mass balance is

$$WR_D = V\frac{dC}{dt} + qC, \tag{1}$$

where R_D is the net rate of desorption (moles/g cat-s), and V the gas-phase volume (cm^3). It is more convenient to convert the gas-phase concentration C to mole fraction y, taking into account the variation of volume flow rate q with temperature T,

$$WR_D = V\beta\frac{P_T}{R}\left\{\left(\frac{dy}{dT}\right)\frac{1}{T} - \frac{y}{T^2}\right\} + \frac{q_0 P_T}{RT_0}y, \tag{2}$$

where we have also, for dissociative adsorption,

$$R_D = -0.5H\frac{d\theta}{dt}. \tag{3}$$

Here, β is a linear heating rate (K/s), P_T the total pressure (1 atm), R the universal gas constant, q_0 the volume flow rate (ambient) (cm^3/s), T_0 the room temperature (K), and H the number of moles of sites/g cat. The kinetics of adsorption/desorption is represented by

$$-\frac{d\theta}{dt} = k_d(\theta, T)\theta^2 - k_a(\theta, T)y(1 - \theta)^2, \quad (4)$$

where Eq. (4) is for a second-order (dissociative) process. k_a and k_d are the rate constants for the adsorption and desorption elementary steps (s^{-1}), respectively, and θ is the fractional coverage of adsorption sites. We can combine Eqs. (2)–(4) and obtain a complete description of the process. However, it can be shown (see results of Table 4) that it is quite justifiable to neglect the accumulation term in Eq. (2) compared to the effluent term. Thus Eq. (2) becomes

$$WR_D = \frac{q_0 P_T}{RT_0} y. \quad (5)$$

Then Eqs. (3)–(5) give

$$y = \frac{0.5WHk_d\theta^2}{\left\{\frac{q_0P_T}{RT_0} + 0.5k_a(1 - \theta)^2WH\right\}}. \quad (6)$$

The second simplification made is to consider that the rate of readsorption is much larger than the rate of removal of the adsorbate from the reactor. This is equivalent to neglecting the term q_0P_T/RT_0 compared to $0.5k_a(1 - \theta)^2WH$, so that we get

$$y = \frac{k_d\theta^2}{k_a(1 - \theta)^2} = \frac{\theta^2}{K(1 - \theta)^2}, \quad (7)$$

with K (thermodynamic equilibrium constant) defined as

$$K(\theta, T) = \frac{k_a}{k_d}, \quad (8)$$

since the reversible adsorption/desorption can be considered as an elementary reaction. Equation (7) is the only relationship needed for the analysis of a series of experimental TPDs (with different initial coverages) in order to extract $\Delta H°(\theta)$ and $\Delta S°(\theta)$. The thermodynamic equilibrium constant K is given by

$$K = \exp(\Delta S°/R)\exp(-\Delta H°/RT). \quad (9)$$

To find out whether q_0P_T/RT_0 in Eq. (6) is small compared to $0.5k_a(1 - \theta)^2WH$, an estimate of k_a is needed. Via the kinetic theory of gases and using mole fraction y instead of concentration C for the gas-phase composition, k_a is given by

$$k_a = S_0\sigma\left(\frac{R}{2\pi M}\right)^{0.5}\left(\frac{P_T}{R}\right)N_A\left(\frac{1}{T}\right)^{0.5}, \quad (10)$$

where σ is the surface metal atom cross-sectional area (cm^2), M the molecular weight of adsorbate (g/mol), and N_A the Avogadro's number. Data on a number of single-crystal surfaces, for a nonactivated adsorption, suggest the sticking coefficient to be $S_0 > 0.01$ (*45*). We do not assume the value of S_0, but instead S_0 is left as a parameter to be calculated such that the ratio of the effluent and readsorption terms is within ca. 5% (reasonable experimental range). It should be expected that S_0 for supported metals should be equal to or greater than S_0 for a flat surface (*45*).

ACKNOWLEDGMENTS

Support of this work was provided by the National Science Foundation through Grant No. CBT-8517158 and by the University of Connecticut Research Foundation.

REFERENCES

1. Cvetanovic, R. J., and Amenomiya, Y., *in* "Advances in Catalysis" (D. D. Eley, H. Pines, and P. B. Weisz, Eds.), Vol. 17, p. 103. Academic Press, New York, 1967.
2. Falconer, J. L., and Schwarz, J. A., *Catal. Rev. Sci. Eng.* **25,** 141 (1983).
3. King, D. A., *Surf. Sci.* **47,** 384 (1975).
4. Bauer, E., Bonczek, F., Poppa, H., and Todd, G., *Surf. Sci.* **53,** 87 (1975).
5. Habenschaden, E., and Kuppers, J., *Surf. Sci.* **138,** L147 (1984).
6. Redhead, P. A., *Vacuum* **12,** 203 (1962).
7. Chan, C.-M., Aris, R., and Weinberg, W. H., *Appl. Surf. Sci.* **1,** 360 (1978).
8. Goymour, C. G., and King, D. A., *J. Chem. Soc. Faraday Trans. 1* **69,** 749 (1973).

9. Cassuto, A., and King, D. A., *Surf. Sci.* **102,** 388 (1981).
10. Adams, D. L., *Surf. Sci.* **42,** 12 (1974).
11. Rieck, J. S., and Bell, A. T., *J. Catal.* **85,** 143 (1984).
12. Gorte, R. J., *J. Catal.* **75,** 164 (1982).
13. Demmin, R. A., and Gorte, R. J., *J. Catal.* **90,** 32 (1984).
14. Brenner, A., and Hucul, D. A., *J. Catal.* **56,** 134 (1979).
15. Ibok, E. E., and Ollis, D. F., *J. Catal.* **66,** 391 (1980).
16. Balkenende, A. R., Geus, J. W., Kock, A. J. H. M., and Van der Pas, R. J., *J. Catal.* **115,** 365 (1989).
17. Chin, A. A., and Bell, A. T., *J. Phys. Chem.* **87,** 3482 (1983).
18. Bertucco, A., and Bennett, C. O., *Appl. Catal.* **35,** 329 (1987).
19. Lee, P. I., and Schwarz, J. A., *J. Catal.* **73,** 272 (1982).
20. Weatherbee, G. D., and Bartholomew, C. H., *J. Catal.* **87,** 55 (1984).
21. Efstathiou, A. M., and Bennett, C. O., *Chem. Eng. Comm.* **83,** 129 (1989).
22. Efstathiou, A. M., PhD thesis, University of Connecticut, 1989.
23. Hurlbut, C. S., "Dana's manual of Mineralogy," 18th ed., pp. 130–136. Wiley, New York, 1971.
24. Stockwell, D. M., Chung, J. S., and Bennett, C. O., *J. Catal.* **112,** 135 (1988).
25. Stockwell, D. M., and Bennett, C. O., *J. Catal.* **110,** 354 (1988).
26. (*a*) Efstathiou, A. M., and Bennett, C. O., *J. Catal.* **120,** 118 (1989); (*b*) Efstathiou, A. M., and Bennett, C. O., *J. Catal.* **120,** 137 (1989).
27. Scholten, J. J. F., Pijpers, A. P., and Hustings, A. M. L., *Catal. Rev.-Sci. Eng.* **27**(1), 151 (1985).
28. Edwards, S. M., Gasser, R. P. H., Green, D. P., Hawkins, D. S., and Stevens, A. J., *Surf. Sci.* **72,** 213 (1978).
29. Zakumbaeva, G. D., and Omashev, K. G., *Kinet, Catal.* **18,** 379 (1977).
30. Cruco, A., Degols, L., Lienard, G., and Frennet, A., *Acta Chim. Acad. Sci. Hung.* **111**(4), 547 (1982).
31. Feulner, P., and Menzel, D., *Surf. Sci.* **154,** 465 (1985).
32. Yates, J. T., Thiel, P. A., and Weinberg, W. A., *Surf. Sci.* **84,** 427 (1979).
33. Christmann, K., Ertl, G., and Pignet, T., *Surf. Sci.* **54,** 365 (1976).
34. Horlacher Smith, A., Barker, R. A., and Estrup, P. J., *Surf. Sci.* **136,** 327 (1984).
35. Chan, C.-M., Thiel, P. A., Yates, J. T., and Weinberg, W. H., *Surf. Sci.* **76,** 296 (1978).
36. Behm, R. J., Christmann, K., and Ertl, G., *Surf. Sci.* **99,** 320 (1980).
37. Gorodetskii, V. V., Nieuwenhuys, B. E., Sachtler, W. M. H., and Boreskov, G. K., *Surf. Sci.* **108,** 225 (1981).
38. Matyi, R. J., Schwartz, L. H., and Butt, J. B., *Catal. Rev.-Sci. Eng.* **29**(1), 41 (1987).
39. Underwood, R. P., and Bell, A. T., *J. Catal.* **109,** 61 (1988).
40. Vannice, M. A., Hyun, S. H., Kalpakci, B., and Liauh, W. C., *J. Catal.* **56,** 358 (1979).
41. Mimeault, V. J., and Hansen, R. S., *J. Chem. Phys.* **45**(6), 2240 (1966).
42. Ponec, V., and van Barneveld, W. A., *Ind. Eng. Chem. Prod. Res. Dev.* **18**(4), 268 (1979).
43. Watson, P. R., and Somorjai, G. A., *J. Catal.* **74,** 282 (1982).
44. Castner, D. G., Sexton, B. A., and Somorjai, G. A., *Surf. Sci.* **71,** 519 (1978).
45. Somorjai, G. A., *in* "Chemistry in Two Dimensions, Surfaces." Cornell Univ. Press, Ithaca, NY, 1981.